DATED HISTORY

Condensed Scalar Geometry: Observable Spacetime as a Sheaf of Timing Closures

May proposal connecting scalar timing and sheaf geometry. The subsequent source/window audit restored closure in zero of nine cases. Curvature requires independent connection data.

Manuscript · p. 1, central thesis

A Test Protocol for Scalar Timing Closure and Dimensional Selection

Evidence · Scalar source/window residual audit

Condensed Scalar Geometry

Observable Spacetime as a Sheaf of Timing Closures

Joshua Farrow

Draft 0.2 - May 2026

Central thesis

Spacetime is not first a manifold. It is the stable global section of compatible scalar timing observations over a category of finite relational probes.

Status: theoretical synthesis and numerical research program. The numerical results reported here are internal closure tests, not experimental evidence for new spacetime dynamics.

Abstract

This paper proposes Condensed Scalar Geometry as a mathematical and physical framework for treating observable spacetime not as a primitive manifold, but as the stable global section of compatible scalar timing observations over a category of finite relational probes. The framework unifies prior scalar-selection, scalar timing, numerical closure, external-kernel, and QATNU/SRQID-style relational programs. It begins from a microscopic or mesoscopic relational substrate and assigns to each admissible probe context a weighted graph, a graph Laplacian, a scalar load field, an effective timing law, and a possible internal-to-external coupling kernel. The leading scalar closure is (kappa L_w + mu^2 I)Lambda = A rho, and the timing readout is omega_eff = omega/(1 + alpha Lambda). Earlier work identified the core closure criterion: the same operator must support diffusion dimension, shell-profile scalar dimension, and timing-law fit in the same scaling window. Condensed Scalar Geometry adds a fourth requirement: local scalar timing data must glue across overlapping probe contexts with low residual. Geometry is therefore not identified with any one graph, field, or embedding. It is identified with the compatibility class of scalar timing closures.

First-pass numerical experiments support the internal coherence of the proposal. On regular graph probes, the diffusion estimator gives d_eff approximately 1.05, 2.04, and 2.93 for 1D, 2D, and 3D branches respectively, while the 3D shell estimator gives d_eff^(Lambda) approximately 3.08, recovering the inverse-radius scalar branch. Local patch gluing residuals fall sharply with screening/locality, from roughly 0.54 at mu = 0.10 to 0.09 at mu = 1.20, while incompatible-patch controls remain near 1.96. A synthetic timing recovery test recovers alpha = 0.25 with RMS fractional residual near 10^-4. These results are not physical evidence for new spacetime dynamics; they are evidence that closure, dimension, timing, and gluing tests form a coherent and falsifiable numerical program.

The paper does not claim full tensor gravity, universal external scalar fields, antigravity, or a completed theory of quantum gravity. Instead, it defines a stricter object: a scalar-timing sheaf over relational probes, whose successful gluing would be the first observable shadow of emergent geometry.

Contents

1. Introduction: the object was wrong
2. The old papers as one program
3. The new primitive: scalar-timing assignments over probes
4. Probe contexts and the scalar observation functor
5. The sheaf principle: geometry as gluing
6. Scalar closure, timing, and the first observable geometry
7. Dimensional selection and the inverse-radius branch
8. Numerical evidence: first-pass internal tests
9. QATNU/SRQID as one possible generator
10. External kernels and experimental posture
11. The full closure score
12. Failure modes and falsifiability
13. Research program
14. Conclusion

Appendix A. Minimal numerical protocol

Appendix B. Definitions and notation

References

1. Introduction: the object was wrong

A theory can fail not because its equations are poor, but because its primitive object is wrong.

Classical geometry begins with a space. General relativity begins with a differentiable manifold equipped with a metric tensor. Quantum information approaches often begin with a Hilbert space, a graph, a tensor network, or a cellular automaton. Earlier versions of the scalar-selection program began with a promoted weighted graph and asked whether a scalar timing sector could emerge from it. That was already a step away from manifold-first thinking, but it left one ambiguity unresolved: is the graph itself the geometry, or is the graph merely one observational chart?

The shift

The graph is not the world. The scalar field is not the world. The clock readout is not the world. The world is the compatible gluing of many such readouts.

Condensed Scalar Geometry takes the second view. The graph is a probe-context, not the final ontology. A scalar solution on a graph is a local report, not yet a spacetime. A clock shift is a timing observation, not yet a metric. The geometry is the stable object reconstructed when these reports agree across refinements, restrictions, overlaps, and alternative readouts.

The inspiration is partly mathematical. In condensed mathematics, Clausen and Scholze replace ordinary topological spaces with sheaf-like objects on profinite test spaces, producing a framework in which topology and algebra interact more cleanly than they do in the ordinary category of topological spaces. The present paper does not import that machinery wholesale. It borrows the deeper discipline: do not assume that the familiar space is the primitive. Define the test contexts, define the observable assignment, and let the global object be what glues.

This is also the lesson of Chandrasekhar's shock at the Kerr solution. Kerr did not provide a vague metaphor for black holes; it supplied a compact exact form that nature could instantiate. The scalar-selection program needs the same severity. Its Kerr-like object is not a dramatic device or speculative force. It is the smallest mathematical form in which local scalar timing data become globally compatible.

2. The old papers as one program

The prior work can be read as a set of fragments around one emerging object.

Prior component	What it contributed
Scalar Selection: A Research Program for Emergent Timing Geometry	Defined the weighted graph spine, screened scalar closure, timing law, dimensional-selection criterion, microscopic route, and experimental discriminants.
Numerical Closure Tests for Scalar Projection and Dimensional Selection	Converted the conceptual spine into pass/fail tests: diffusion dimension, shell dimension, timing residuals, static closure, modal dynamics, and finite-size criteria.
External Coupling Kernels for Internal Scalar Loads	Separated internal scalar load from external measurable response and classified kernel classes: near-field, substrate-mediated, radiative, vacuum-like, and null.
Selection, Projection, and Scalar Emergent Geometry	Framed the observable world as a selected and projected sector of a richer lawful substrate; emphasized timing and propagation before full metricity.
SRQID/QATNU testbed paper	Provided one candidate microscopic generator: unitary local dynamics with clocks coupled to entanglement-carrying bond registers.

Table 1. Prior papers as components of a single closure program.

The old scalar-selection spine was:

```
H_micro -> W -> L_w -> d_eff -> G_d_eff(r) -> Lambda(r) -> omega_eff
```

That chain treated scalar emergent geometry as the first robust observable sector surviving coarse graining and selection. It was already level-aware: microscopic Hamiltonians, mesoscopic weighted graphs, effective scalar loads, external probe kernels, timing shifts, and experimental readouts were not collapsed into one undifferentiated claim. But the chain was still a pipeline. The new paper turns that pipeline into an observable assignment.

Old form vs. new form

Old: geometry is a scalar field on a promoted graph. New: geometry is a compatible family of scalar timing closures over probe contexts.

3. The new primitive: scalar-timing assignments over probes

The primitive object of Condensed Scalar Geometry is not a manifold, not a graph, not a tensor network, and not a scalar field alone. It is a rule assigning scalar timing data to admissible probe contexts, together with a gluing criterion.

```
S : Probe^op -> Obs
```

Here Probe is a category of observational contexts, and Obs is a category of scalar closure data. The contravariance means that a refinement or restriction of a probe context induces a restriction of observable data. In plain language: if a larger setup gives a scalar timing field, each smaller overlapping setup should inherit the relevant part of that field. Conversely, local reports should be assembled only when they agree on overlap.

This simple change prevents three common mistakes. First, it prevents identifying one graph with spacetime. Second, it prevents interpreting one scalar field as full gravity. Third, it prevents internal medium observables from being mistaken for external geometry without a measured or bounded coupling kernel.

Definition: Condensed Scalar Geometry

A Condensed Scalar Geometry is an approximate sheaf-like assignment of scalar closure and timing data to admissible relational probe contexts. Its global spacetime-like content is the family of sections that glue stably under refinement, restriction, and measurement change.

4. Probe contexts and the scalar observation functor

Let Probe denote a category of admissible observational contexts. An object P in Probe is a finite or profinite probe context:

```
P = (G_P, S_P, I_P, epsilon_P)
```

where G_P = (V_P, E_P, w_P) is the effective graph accessible to that probe, S_P is the set of clocks, sensors, or readout channels, I_P is the allowed intervention class, and epsilon_P is the resolution or coarse-graining scale. A morphism f: Q -> P represents refinement, restriction, coarse-graining, subgraph inclusion, change of readout, or another observational cut.

For each probe context P, the scalar observation assignment gives:

```
S(P) = (W_P, L_w,P, rho_P, Lambda_P, omega_eff,P, C_P)
```

The weighted graph Laplacian is

```
L_w,P = D_P - W_P
```

and the local scalar closure is

$$(\kappa L_{w,P} + \mu^2 I)\,\Lambda_P = A\,\rho_P$$

The timing readout is

$$\omega_{\mathrm{eff},P} = \omega / (1 + \alpha \Lambda_P)$$

and in weak load

$$\delta\omega / \omega \approx -\alpha \Lambda_P$$

The old scalar timing law is preserved. What changes is its interpretation. It is no longer the field on the graph. It is one local section of an observable assignment.

5. The sheaf principle: geometry as gluing

Suppose a probe context P is covered by smaller contexts $\{P_i \to P\}$. Each context gives local scalar timing data s_i in $S(P_i)$. These local data are compatible only if they agree on overlaps:

$$s_i|_{(P_i \cap P_j)} = s_j|_{(P_i \cap P_j)}$$

When they agree, there should exist a global section s in S(P) such that

$$s|_{(P_i)} = s_i$$

for all i. In exact mathematics, this is a strict sheaf condition. In physics, every measurement is finite-resolution, noisy, screened, and coarse-grained. Therefore Condensed Scalar Geometry replaces exact equality with a quantitative gluing residual.

$$R_{\mathrm{glue}} = \sum_{ij} \| s_i|_{\mathrm{overlap}} - s_j|_{\mathrm{overlap}} \| \,/\, \sum_{ij} (\|s_i|_{\mathrm{overlap}}\| + \|s_j|_{\mathrm{overlap}}\|)$$

Core physical interpretation

A geometry exists when many local timing closures can be assembled into one stable scalar timing section without contradiction.

This turns curvature, screening, topology, and externalization into compatibility questions. Flat scalar geometry corresponds to low-residual gluing. Curvature corresponds to systematic mismatch between local closures. Screening corresponds to loss of gluing strength with distance. Topology change corresponds to inequivalent global sections arising from locally compatible data. Decoherence corresponds to unstable gluing under refinement. Externalization corresponds to a nontrivial map from internal scalar sections to external sensor sections.

6. Scalar closure, timing, and the first observable geometry

The leading scalar closure

$$(\kappa L_w + \mu^2 I)\Lambda = A\rho$$

is the lowest-order local, linear, positive, graph-symmetric response compatible with weak superposition. It can also be understood as the Euler-Lagrange equation of a quadratic roughness-plus-screening functional:

$$F[\Lambda] = \frac{\kappa}{2}\langle \Lambda, L_w \Lambda \rangle + \frac{\mu^2}{2}\|\Lambda\|^2 - \langle \rho, \Lambda \rangle$$

This is not asserted as the final law of nature. It is the leading closure whose failure can be measured. Nonlinear terms, higher Laplacian powers, memory kernels, and tensorial sectors belong to later layers of the theory.

The timing law

$$\omega_{eff} = \omega / (1 + \alpha \Lambda)$$

says that scalar load is first read as a frequency shift. The operational observable is therefore not force but timing. This preserves the strongest claim of the earlier work: scalar timing is not necessarily deeper than gravity in an ontological sequence, but it may be easier to read. It is the first stable shadow of geometry available to clocks.

7. Dimensional selection and the inverse-radius branch

The same weighted Laplacian that defines scalar response also defines diffusion. With heat kernel $K(t) = \exp(-t L_w)$, the return probability is

$$P_{return}(t) = (1/|V|) \operatorname{Tr} K(t)$$

and the diffusion-based effective dimension is

$$d_{eff}^{(diff)}(t) = -2 \frac{d \log P_{return}(t)}{d \log t}$$

Independently, a shell-averaged scalar load around a source gives a shell estimator. In a Gaussian scaling regime,

$$\Lambda_{shell}(r) \sim G_{d_{eff}}(r) \sim r^{(2 - d_{eff})}, \quad d_{eff} \neq 2$$

Hence

$$d_{eff}^{(\Lambda)}(r) = 2 - \frac{d \log |\Lambda_{shell}(r)|}{d \log r}$$

The severe scalar-selection test is not that either estimator works alone. It is that both estimators agree in the same scaling window where the timing law fits best:

$$d_{eff}^{(diff)} \approx d_{eff}^{(\Lambda)} \approx 3$$

When d_{eff} is approximately 3, the Green branch becomes

$$\Lambda(r) \sim 1/r$$

and the timing law gives

$$\frac{\delta \omega}{\omega} \sim -1/r$$

This reproduces the radial envelope of weak-field gravitational redshift without assuming an ordinary three-dimensional manifold at the foundation. Condensed Scalar Geometry adds the gluing condition: the inverse-radius branch matters only if local scalar timing closures also assemble into stable global sections.

Scalar-timing dimensional closure

If a probe family admits a common weighted-Laplacian operator, a Gaussian scaling window, agreement of diffusion and shell estimators near three, low timing residual, and low gluing residual across overlapping contexts, then it supports a scalar-timing geometry with an inverse-radius weak-field branch.

8. Numerical evidence: first-pass internal tests

The first numerical tests evaluate internal coherence, not physical truth. They ask whether the proposed closure criteria can be implemented and whether the expected branch structure appears in simple graph families.

8.1 Dimension closure

Probe branch	Diffusion estimate	Shell estimate	Interpretation
1D regular branch	1.047 +/- 0.034	not used	not Newton-like
2D regular branch	2.045 +/- 0.078	logarithmic branch	critical/log regime

3D regular branch	2.933 +/- 0.140	3.077 +/- 0.148	inverse-radius scalar window

Table 2. First-pass dimension closure summary from regular graph probes.

The 3D branch is the important result. The same operator supports a diffusion dimension near three and a shell response consistent with the 1/r branch. This does not prove that the universe selects d = 3. It shows that the numerical closure pipeline behaves as predicted when the correct branch is present.

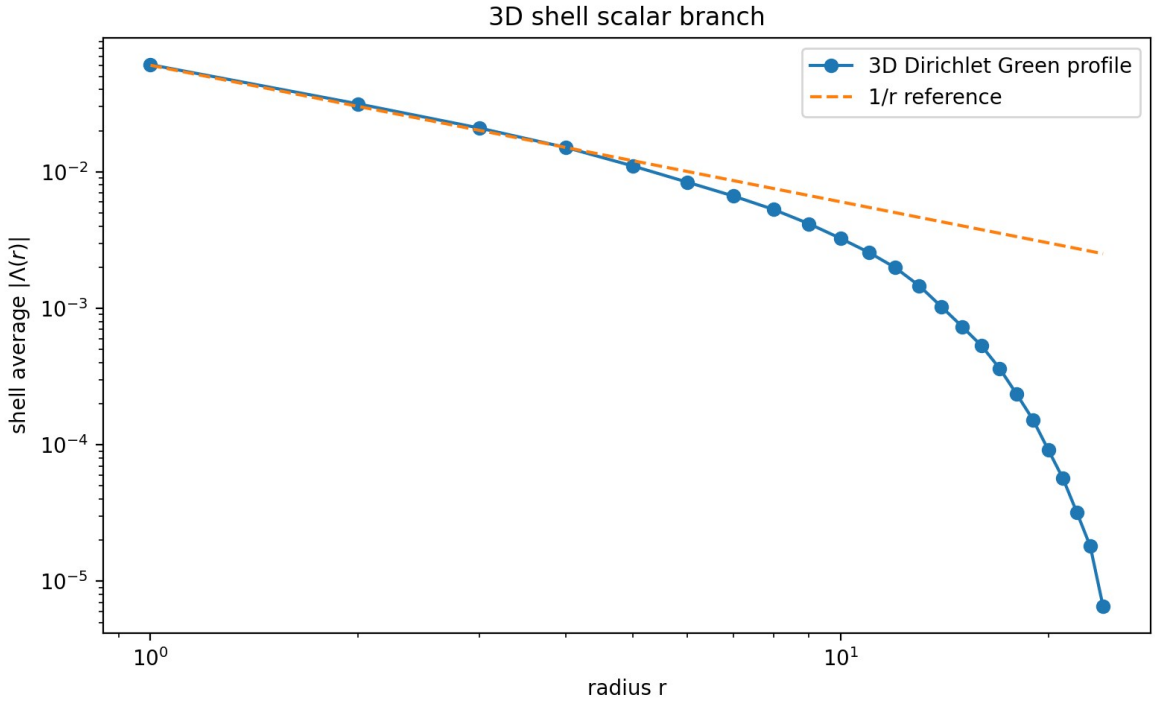

Figure 1. 3D shell scalar profile. The measured shell average follows the inverse-radius branch over the useful interior window before finite-boundary effects dominate.

8.2 Gluing closure

A 3D graph was covered with overlapping finite probe patches. The scalar closure was solved locally on each patch, and patch agreement was measured on overlaps. For patch radius R = 3, the residuals were:

Screening scale mu	Overlap gluing residual
0.10	0.537
0.20	0.485
0.35	0.391
0.60	0.256
0.80	0.182
1.00	0.130
1.20	0.094

Table 3. Local scalar closure gluing residual decreases as screening/locality increases.

The incompatible-patch control residual was approximately R_incompatible = 1.964. Thus local scalar closures do not automatically glue. They glue when locality and screening make overlap agreement possible.

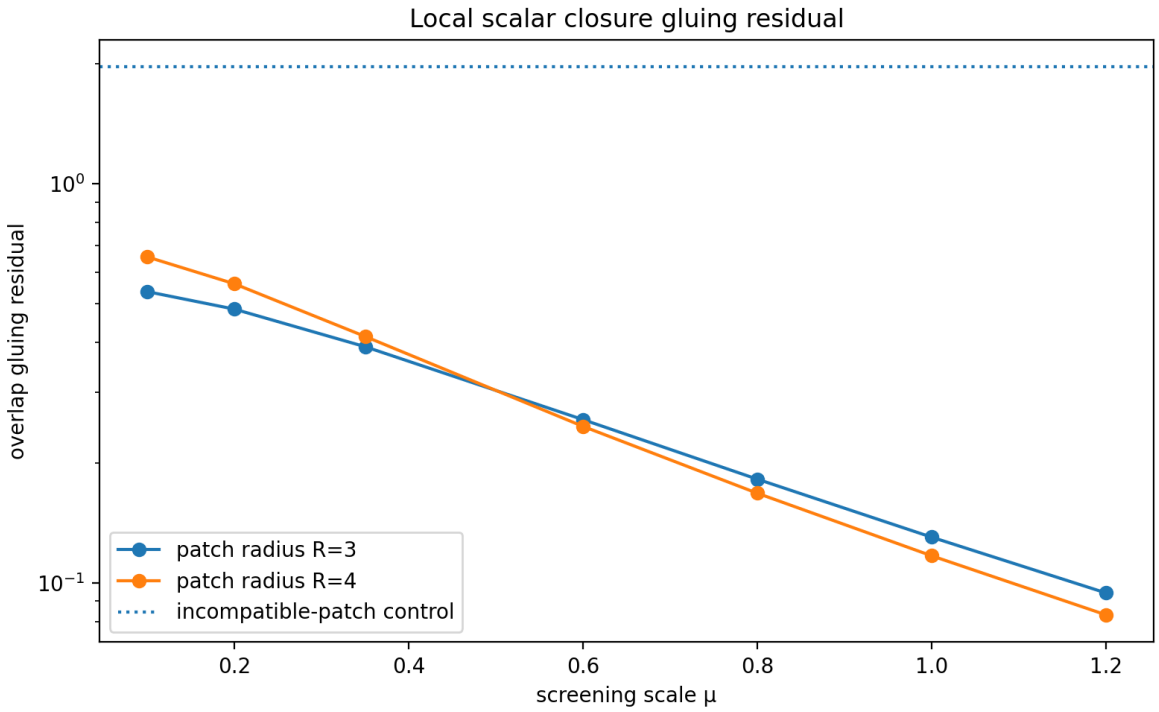

Figure 2. Local scalar closure gluing residual as a function of screening scale. The incompatible-patch control remains far above coherent scalar closure runs.

8.3 Timing-law recovery

Synthetic noisy clock data were generated from the scalar field with alpha_true = 0.25. A scan over alpha recovered alpha_fit = 0.25 with RMS fractional residual near 1.0 x 10^-4. This confirms that the timing parameter can be recovered cleanly when scalar load data are available. It is not independent evidence for a real physical scalar field; it validates the measurement logic.

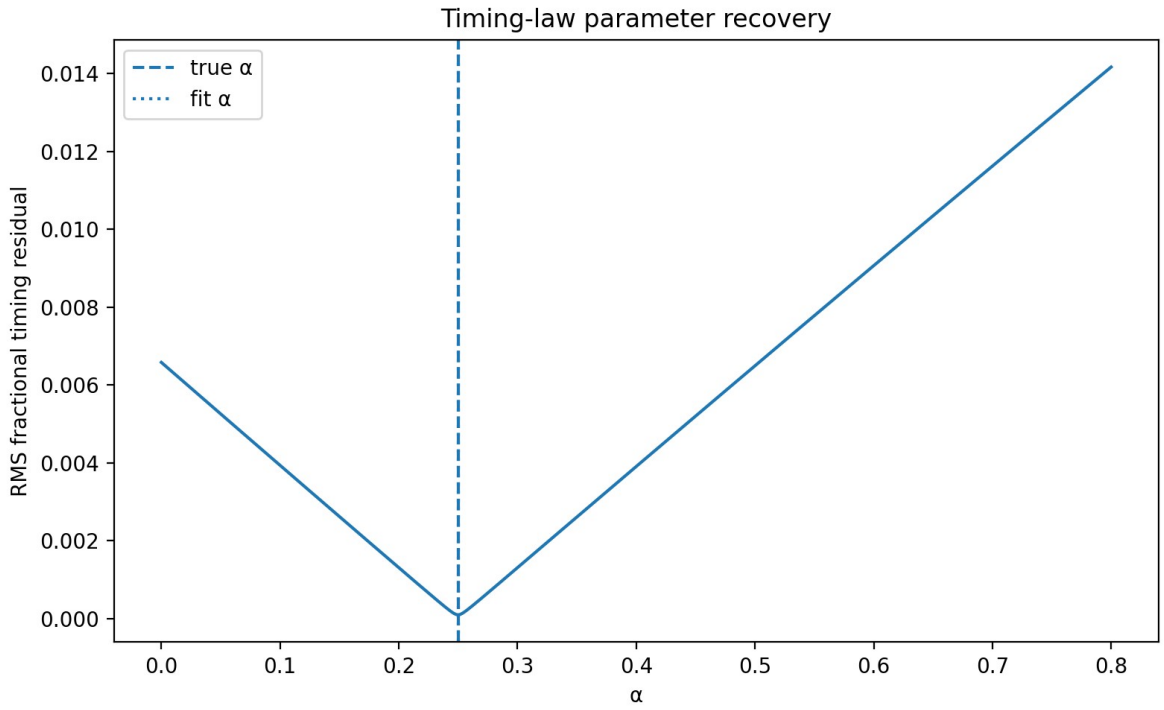

Figure 3. Synthetic timing-law parameter recovery. The residual minimum occurs at the true alpha used to generate the data.

8.4 Interpretation of the numerical evidence

- The dimension closure test is implementable.
- The d_eff approximately 3 branch recovers the inverse-radius scalar profile.
- Approximate sheaf-like gluing can be measured and can fail.
- The timing-law parameter can be recovered under controlled synthetic conditions.

The tests do not establish a physical external scalar field, a tensor gravitational sector, universal spacetime emergence, or a microscopic derivation from a specific experimental substrate. They move the theory from conceptual coherence to internally testable structure.

9. QATNU/SRQID as one possible generator

Condensed Scalar Geometry does not require a single microscopic substrate. It is an observable framework. Still, QATNU/SRQID provides one candidate generator.

The SRQID/QATNU testbed models a unitary, measurement-free quantum cellular automaton in which local matter clocks couple to entanglement-carrying bond registers through frustration-controlled promotion. Its effective timing law has the same form used here:

```
omega_eff = omega / (1 + alpha Lambda)
```

with Lambda interpreted as local entanglement depth or scalar load. This gives a concrete route from microscopic relational dynamics to scalar timing sections. In the new language, QATNU/SRQID is not itself the final spacetime. It is a source of candidate local scalar timing data.

This clarifies the role of the earlier clock-lag work. Scalar timing is not necessarily before gravity in a chronological sense. It is first in a readability sense. Tensor gravity, gauge sectors, and classical records require richer observational algebras. Scalar timing is the minimal stable projection that clocks may be able to read.

10. External kernels and experimental posture

The external-kernel problem is central. An internal scalar load on graph vertices does not by itself imply an external measurable scalar geometry. An external probe at position x measures, at best,

```
Lambda_ext(x) = sum_i C(x,i) Lambda_i
```

The kernel C(x,i) determines whether the scalar sector externalizes, how it decays, and which experimental geometry is appropriate. In Condensed Scalar Geometry, C is a morphism between internal and external observable assignments:

```
S_internal => S_external
```

Kernel class	Distance law	Distinctive signature
Near-field / evanescent	Exponential or short-range	Strong dependence on standoff and substrate thickness
Substrate-mediated diffusive	Material-dependent	Time-delayed and broadened response; dependence on substrate properties
Radiative / boundary-modulated	Resonant or mode-dependent	Frequency-selective enhancement and phase-sensitive readout
Vacuum / effective Green-response	Power law or screened power law	Spatial law not reducible to ordinary substrate coupling
Null	None	Internal sensor sees effect; external sensor sees nothing

Table 4. External kernel classes as candidate maps from internal scalar sections to external observables.

A serious experiment should vary distance, substrate material and thickness, drive frequency, topology at fixed mass, shielding, and cavity boundary conditions. The decisive signature is not merely a shifted clock. Clocks shift for many ordinary reasons. The decisive signature is a timing response whose spatial, temporal, and topological structure follows the scalar closure better than thermal, electromagnetic, mechanical, or mass-redistribution controls.

11. The full closure score

A transient d_eff approximately 3 crossing is not enough. A convincing scalar-timing geometry must satisfy dimension closure, timing closure, gluing closure, finite-size stability, modal dynamics, and external-kernel discrimination in one common regime.

```
C_CSG = w_d R_d + w_t R_t + w_g R_g + w_f R_f + w_m R_m + w_e R_e
```

Term	Definition	Meaning
R_d	|d_eff^(diff) - d_eff^(Lambda)|	Dimension estimator agreement
R_t	timing-law residual	Clock response fit
R_g	gluing residual	Patch compatibility / sheaf-like closure
R_f	finite-size drift	Stability under system size and refinement
R_m	modal-spectrum mismatch	Relaxation rates vs. graph Laplacian spectrum
R_e	external-kernel mismatch	External response vs. kernel class and nuisance controls

Table 5. Components of the Condensed Scalar Geometry closure score.

The theory does not pass because one beautiful equation works. It passes only if dimension, scalar response, timing, gluing, dynamics, and externalization cohere.

12. Failure modes and falsifiability

Condensed Scalar Geometry is designed to fail cleanly. Each failure mode narrows scope while increasing truthfulness.

- Internal closure failure: diffusion and shell dimension estimators do not agree.
- Dimensional failure: the estimators agree but not near the inverse-radius branch.
- Timing failure: the timing law fits in a different window from the dimension closure.
- Gluing failure: local scalar sections do not agree on overlaps.
- Dynamical failure: modal relaxation rates do not track the graph Laplacian spectrum.
- Externalization failure: C(x,i) is null, or observed signals are fully explained by ordinary thermal, electromagnetic, mechanical, or substrate-mediated channels.
- Medium failure: no real medium produces the leading screened weighted-Laplacian closure in a measurable regime.
- Tensor failure: scalar timing closes, but no spin-2 or tensorial sector emerges at larger scale.

The strongest version of the theory survives only if the same promoted operator controls scalar response, effective dimension, timing shift, gluing compatibility, and external measurement in one real scaling window.

13. Research program

The next phase is not to inflate the claim. It is to make the closure tests harsher.

13.1 Numerical expansion

- Run gluing residual tests on path, cycle, diamond, bowtie, star, lattice, random geometric, small-world, and QATNU-derived promoted graphs.
- Measure how R_glue scales with patch size, overlap size, screening scale, source placement, disorder, and graph refinement.
- Test whether low R_d, R_t, and R_g occur in the same scaling window or only separately.
- Add dynamic closure tests by comparing measured relaxation modes to tau_n^-1 = Gamma(kappa lambda_n + mu^2).
- Run finite-size scaling to determine whether apparent d_eff approximately 3 plateaus sharpen or drift away.

13.2 Microscopic derivation

- Derive W, rho, and Lambda from candidate physical media rather than choosing them phenomenologically.
- Use superconducting coupler networks as the first bounded test medium because they provide programmable weighted graphs and sensitive phase readout.
- Separate internal scalar observables from external sensor responses at every step.

13.3 Experimental path

- Begin with an integrated cryogenic phase sensor or spectator qubit as a first-bound internal sensor.
- Move to external optical or microwave timing probes only after internal closure and nuisance channels are quantified.
- Report bounds on alpha A, mu, Gamma, and the kernel class rather than claiming direct spacetime modification.

14. Conclusion

Condensed Scalar Geometry proposes a new primitive for emergent spacetime research. Not a manifold. Not a graph. Not a tensor network. Not a scalar field alone. The primitive is a sheaf-like scalar timing assignment over admissible relational probes.

Final thesis

Spacetime is the stable global section of compatible scalar timing observations.

The current evidence is preliminary but meaningful. The scalar-selection spine already provided the operator closure, timing law, dimensional-selection criterion, and experimental caution. First-pass numerical tests now show that the d_eff approximately 3 branch recovers the inverse-radius scalar profile, that local scalar closures can be tested for gluing, and that the timing-law parameter can be recovered under controlled conditions.

What remains is the hard work: larger graph families, QATNU-derived promoted graphs, irregular and random relational substrates, finite-size scaling, modal relaxation tests, and real-medium kernel bounds. The theory will either find a scaling window where dimension, timing, gluing, and externalization cohere, or it will narrow itself. Either result is progress. The goal is not to win by metaphor. The goal is to find the form nature can actually use.

Appendix A. Minimal numerical protocol

Step	Operation
1	Choose or extract a promoted weighted graph W.
2	Compute L_w = D - W.
3	Compute return probability P_return(t) = |V|^-1 Tr exp(-t L_w).
4	Estimate d_eff^(diff)(t).
5	Solve (kappa L_w + mu^2 I)Lambda = A rho.
6	Form shell averages Lambda_shell(r).
7	Estimate d_eff^(Lambda)(r).
8	Fit omega_eff = omega/(1 + alpha Lambda) and record timing residual.
9	Cover the graph by overlapping patches and compute R_glue.
10	If time-resolved data exist, fit relaxation modes and compare with L_w eigenvalues.
11	Repeat over system sizes, thresholds, source placements, topologies, and kernel hypotheses.

Table A1. Minimal numerical workflow for CSG closure tests.

Appendix B. Definitions and notation

Symbol	Meaning
H_micro	Microscopic Hamiltonian or relational substrate dynamics
W	Weighted adjacency / coupling matrix
L_w	Weighted graph Laplacian D - W
rho	Effective source density
Lambda	Internal scalar load
Lambda_ext	External scalar load at sensor position
C(x,i)	Internal-to-external coupling kernel
kappa	Scalar transport / stiffness coefficient
mu	Screening scale
A	Source amplitude coefficient
Gamma	Relaxation-rate coefficient
d_eff	Effective spectral dimension
omega	Bare clock frequency
omega_eff	Effective local frequency
alpha	Clock susceptibility to scalar load
R_glue	Failure of local scalar sections to agree on overlaps
S : Probe^op -> Obs	Scalar timing assignment over probe contexts

Table B1. Condensed Scalar Geometry notation.

References

Bothwell, T. et al. (2022). Resolving the gravitational redshift across a millimetre-scale atomic sample. Nature 602, 420-424.

Burioni, R. and Cassi, D. (1996). Universal properties of spectral dimension. Physical Review Letters 76(7), 1091-1093.

Chung, F. and Yau, S.-T. (2000). Discrete Green's functions. Journal of Combinatorial Theory A 91(1-2), 191-214.

Clausen, D. and Scholze, P. (2026). Condensed Mathematics and Complex Geometry. Lecture notes.

Farrow, J. (2025). Self-Referential Quantum Information Dynamics as a Discrete Testbed for Emergent Gravity: Results, Anchors, and Limitations. Internal draft.

Farrow, J. (2026a). Scalar Selection: A Research Program for Emergent Timing Geometry. Internal draft.

Farrow, J. (2026b). Numerical Closure Tests for Scalar Projection and Dimensional Selection. Internal note.

Farrow, J. (2026c). External Coupling Kernels for Internal Scalar Loads. Internal note.

Farrow, J. (2026d). Selection, Projection, and Scalar Emergent Geometry: Toward a Physics of Surviving Observable Worlds. Internal draft.

Kakaes, K. (2026). Two Researchers Are Rebuilding Mathematics From the Ground Up. Quanta Magazine, May 20, 2026.

Lieb, E. H. and Robinson, D. W. (1972). The finite group velocity of quantum spin systems. Communications in Mathematical Physics 28, 251-257.

Scholze, P. (2026). Lectures on Condensed Mathematics. Updated lecture notes.

Schwarz, S., Sturm, A., and Wardetzky, M. (2025). Heat kernel asymptotics for scaling limits of isoradial graphs. Potential Analysis 63, 57-76.